Geoderma 290 (2017) 1–9

Contents lists available at ScienceDirect

Geoderma

journal homepage: www.elsevier.com/locate/geoderma

Why was iron lost without significant isotope fractionation during the lateritic process in tropical environments?

Miao Li [a], Yong-Sheng He [b], Jin-Ting Kang [a], Xiao-Yong Yang [a], Zhi-Wei He [a], Hui-Min Yu [a], Fang Huang [a,*]

[a] CAS Key Laboratory of Crust-Mantle Materials and Environments, School of Earth and Space Sciences, University of Science and Technology of China, Hefei 230026, China
[b] State Key Laboratory of Geological Processes and Mineral Resources, China University of Geosciences, Beijing 100083, China

ARTICLE INFO

Article history:
Received 7 May 2016
Received in revised form 16 September 2016
Accepted 2 December 2016
Available online xxxx

Keywords:
Tropical weathering
Laterite
Iron isotope
Fe cycling

ABSTRACT

To investigate the formation of laterites and Fe cycling during tropical weathering, this study presents Fe isotope and major trace-element compositions of a laterite profile obtained from an equatorial rainforest, Southern Philippines. The lateritic profile is 7 m deep from top soil to less-weathered peridotites. X-ray diffraction analyses reveal that the major Fe-bearing minerals are hematite and goethite. The profile shows a large variation in Fe_2O_3 concentrations (32.1–73.3 wt%) and dramatic Fe loss based on $\tau_{Ti,Fe}$ factors ($\tau_{Ti,Fe} \approx -50\%$ to -90%) calculated from the open-system mass fraction transport function. Notably, $\delta^{56}Fe$ depicts a small range from $-0.03‰$ in the peridotite to $+0.10‰$ in the extremely weathered saprolites.

The small Fe isotopic fractionation and significant Fe loss provide important insights into Fe cycling during extreme weathering of peridotites in a tropical climate. Variations in Fe content and $\delta^{56}Fe$ can be modeled by a Rayleigh distillation process with apparently small fractionation factors of $^{56}Fe/^{54}Fe$ between the saprolite and fluid ($10^3 ln\alpha_{saprolite-fluid}$) of 0.01 to 0.20, much smaller than those experimentally determined for reductive dissolution of goethite ($10^3 ln\alpha_{goethite\text{-}Fe(II)} \approx 1.2$; Icopini et al., 2004) and hematite ($10^3 ln\alpha_{hematite\text{-}Fe(II)} \approx 1.3$; Beard et al., 2003). These observations suggest that Fe should have experienced a complete and *in situ* oxidation prior to Fe migration and Fe was probably transferred in the form of colloidal substances. Fe transport over the history of the laterite formation and evolution may not have had a discernible effect on the Fe isotopic composition of the ecosystem.

1. Introduction

Laterites are oxidized Fe-rich soils covering one third of the continents and are drained by half of the continental rivers. They represent a key role in continental evolution, element cycling from the solid earth to the ocean, and development of terrestrial life (Tardy, 1997). It is therefore necessary to understand how they evolve in response to natural and anthropogenic processes. Iron is the fourth most abundant element in the continental crust and is also extremely abundant in laterites, as shown in their characteristic red color due to the large amount of Fe^{3+}. Because Fe isotopes can be fractionated due to redox reaction during weathering and soil formation (Chapman et al., 2009; Fantle and DePaolo, 2004), Fe isotopic composition of soils can provide a useful tool to investigate laterite formation.

Understanding the behavior of Fe isotopes is important to evaluate transport of Fe during laterite formation and the impact on ecosystems. Previous studies on soils indicate that $\delta^{56}Fe$ of bulk soils show a large range from $-0.62‰$ to $+0.72‰$ (Emmanuel et al., 2005; Fantle and DePaolo, 2004; Fekiacova et al., 2013; Poitrasson et al., 2008; Thompson et al., 2007; Wiederhold et al., 2007a, 2007b). These pioneering studies have documented that notable Fe isotopic variation can occur due to reductive loss of Fe during weathering and soil formation (e.g., Bullen et al., 2001; Johnson et al., 2004; Wiederhold et al., 2006; Yesavage et al., 2012). Ligand-promoted dissolution, proton-promoted dissolution, or reductive Fe dissolution, have been proposed as the key process to control the Fe isotopic composition variation in soils (Emmanuel et al., 2005; Fantle and DePaolo, 2004; Liermann et al., 2011; Wiederhold et al., 2006, 2007a). Yesavage et al. (2012) suggested that the notable Fe isotopic fractionation in soils results from different dissolution and precipitation mechanisms. They invoked two models to explain the iron isotopic variations: (i) the fractionation occurs during dissolution process such as ligand-controlled dissolution or dissimilatory iron reduction, both of which preferentially enrich light iron isotopes in solution; (ii) the isotopic fractionation occurs during precipitation process rather than dissolution (Yesavage et al., 2012), which can be explained using a fractionation factor between the retained Fe precipitate and the mobile particles of 0.9987 (Skulan et al., 2002). There were later iron isotope studies on tropical or subtropical laterite profiles (Liu et al., 2014; Poitrasson et al., 2008). Liu et al. (2014) concerned laterites formed from basalt in southern China, while Poitrasson et al. (2008) studied laterites formed from

* Corresponding author.
E-mail address: fhuang@ustc.edu.cn (F. Huang).

http://dx.doi.org/10.1016/j.geoderma.2016.12.003
0016-7061/

granodiorites in Cameroon. Regardless of the different origin of laterites, they both demonstrate limited δ^{56}Fe variations (<0.15‰) of the whole profile with notable Fe loss during laterite formation. Given that redox transport of Fe could significantly fractionate Fe isotopes, it is not clear why Fe isotope fractionation is dramatically different in soils developed under different climates. There is also a lack of understanding for the coupling of limited iron isotope fractionation with dramatic iron loss. To better understand the Fe isotope variations and Fe loss in laterite forming, we conduct a comprehensive Fe isotope study for the laterites forming from weathering of peridotites under tropical climate.

The lateritic profile in this study is from Surigao, South Philippines. Because the climate is of an equatorial type with a mean annual rainfall of ≈3000 mm and a mean annual temperature of 27 °C, chemical weathering is significantly intensified and the laterite samples in this region have undergone extensive weathering. Therefore, laterites in Surigao, South Philippines, provide a good opportunity to study iron isotope fractionation and decipher iron cycling during extreme weathering processes. This is helpful for understanding how Fe is lost from the bedrocks to soil and water and how laterite forms via weathering of peridotites in tropical weather.

In this study, we report the Fe isotopic compositions, major- and trace-element contents of a typical lateritic profile developed from weathering of peridotites in Surigao, South Philippines. The purpose of this study is to understand the different response of Fe isotopes to weathering conditions and to investigate the cycling of Fe in the near-surface environment. We attribute the Fe lost with small Fe isotope variations in the laterite to a complete and in situ oxidation in the profile to the highly oxidized nature of the Surigao followed by migration, probably in the form of colloid substances, during laterite formation under the tropical climate.

2. Geology background and sample description

The laterite in this study formed in a humid, tropical climate due to weathering of peridotites (Fig. 1). Peridotites are a common ultramafic igneous rock containing <45 wt% silica. They are very important because they are the dominant rock of the upper Earth's mantle. The mineral compositions of peridotites are mainly olivine, clinopyroxene, orthopyroxene, and Al-bearing phases that change with increasing depth from plagioclase (<30 km) to spinel (30–70 km) and then to garnet (>70 km). The major Fe-bearing minerals are olivine ($(Mg,Fe)_2SiO_4$) and pyroxene ($(Ca, Na, Fe^{II},Mg)(Cr, Al, Fe^{III}, Mg, Mn, Ti, V)Si_2O_6$). Olivine is essentially free of Fe^{3+} compared with the other mineral phases in peridotites (i.e., pyroxenes), while both ferrous and ferric irons can exist in garnet, spinel, and pyroxene.

The weathering profile is located in Pili Country, Surigao, the capital city of Surigao del Norte Province and 30 km west of Mainit Lake. This region has a mean annual temperature of 27 °C. The highest maximum monthly temperature is 32–33 °C during August to September, and lowest maximum monthly temperature is 22–24 °C during January and February. Annual precipitation in Surigao is ≈3000 mm and most of the precipitation occurs from November to March. Integrated geological and mineralogical studies of the Surigao area can be found in Braxton et al. (2009).

The studied profile consists of peridotites at the bottom to extremely weathered laterites toward the surface (Fig. 2). The topsoil in the upper 50 cm was not sampled to avoid the disruption of vegetation activities onto iron isotopes. Beneath the topsoil, a set of gravel layers has developed. Four samples (Pili-1 to Pili-4) were collected at intervals of around 40 cm from the gravel layer. The gravels are hematite-rich nodules and the X-ray diffraction (XRD) results reveal that this layer

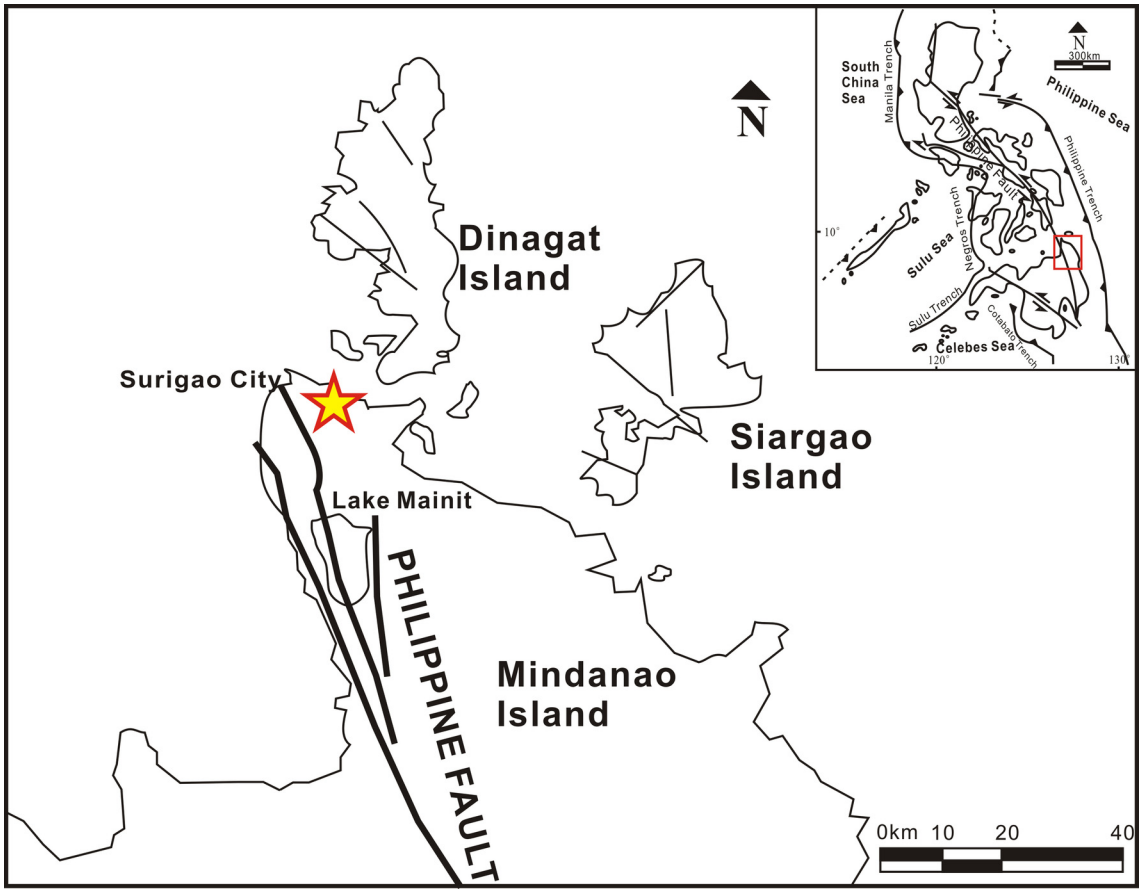

Fig. 1. A simplified geological map for South Philippines with sample location. Star represents sample locality.

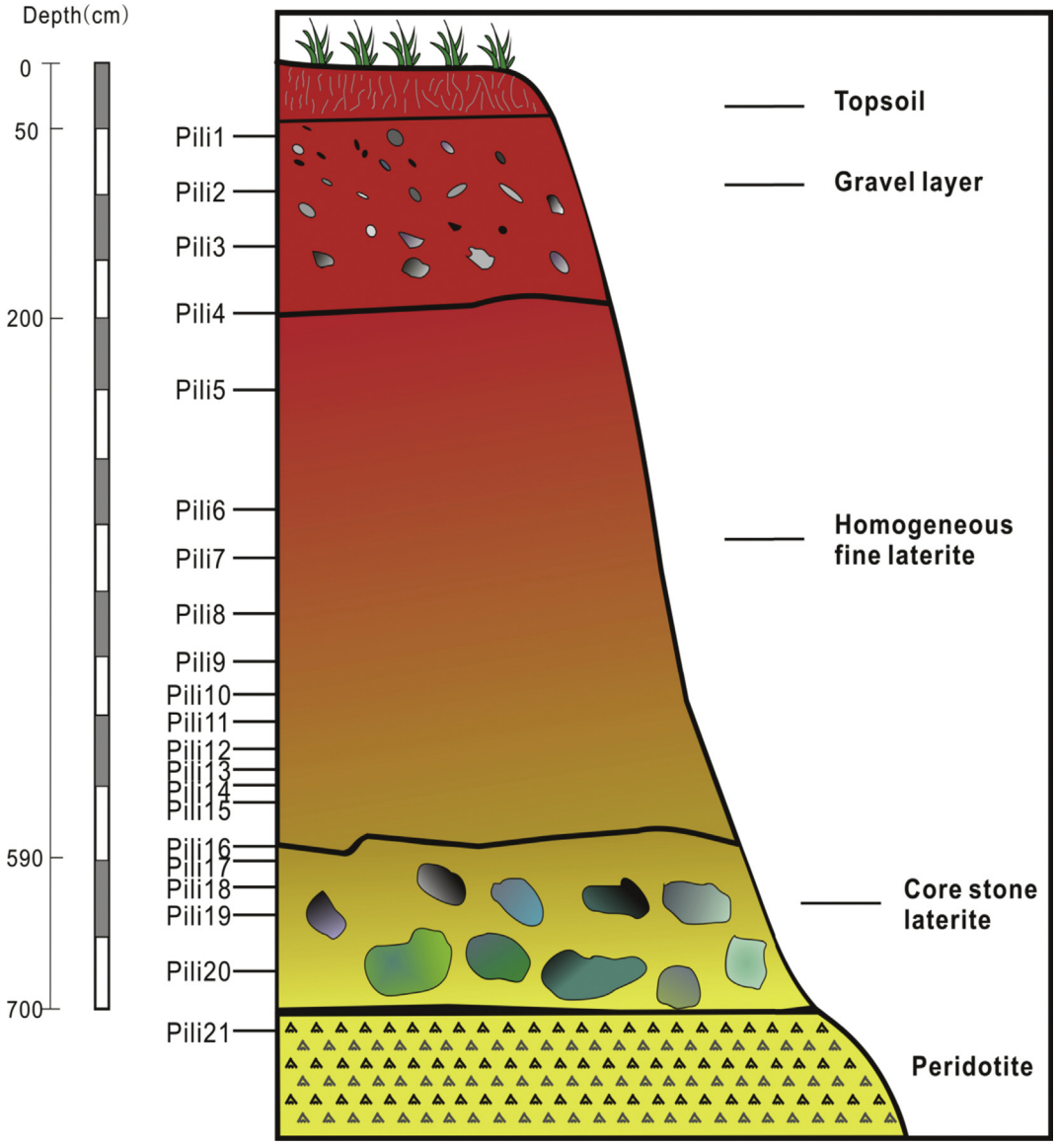

Fig. 2. Sketch section of the peridotite weathering profile in Surigao, South Philippines. According to the texture and color, five different horizons are divided within the profile. Horizontal lines mark the boundaries of each layer. The boundaries between these horizons are gradual. Sample numbers are marked at their sampling positions in the profile.

contains a higher proportion of clay minerals than the other layers. Eleven samples (Pili-5 to Pili-15) were collected in the fine laterite layer with a homogeneous red color from 200 to 590 cm. The soil in this layer is fine in grain size. The soil color turns a little yellowish with the increase in depth, but basically remains red. Four samples were collected from the section below 590 cm, where the soil becomes yellowish with less-weathered core stones with the texture of the original parent rock. Green-yellow serpentinites ($(Mg, Fe^{II},Ni)_3Si_2O_5(OH)_4$) are visible at the lower part of this layer, marking the weathering frontier of peridotites. At a higher level in this layer, rock is soft with dark brownish colors mixed with shades of beige to gray. A peridotite sample (Pili-21) was collected from 7 m below as a representative of base rock (Fig. 2).

3. Analytical methods

Iron isotopic analyses were performed at the Metal Stable Isotope Laboratory of the University of Science and Technology of China (USTC), Hefei, Anhui Province, China. Procedures for sample dissolution, column chemistry, and instrumental analysis are similar to those reported in previous studies (Huang et al., 2011). Briefly, samples were dissolved in a mixture of concentrated HF–HNO_3–HCl in Savillex screw-top beakers. Chemical separation of Fe was achieved by anion exchange chromatography with Bio-Rad 200–400 mesh AG1 X8 resin in a HCl media. Samples containing ~100 μg of Fe were loaded on the resin. Matrix elements were removed by 1.5 ml 6 N HCl, and then Fe can be collected by 4 ml of 0.5 N HCl followed by 1 ml of 8 N HNO_3 and 0.5 ml of H_2O. Fe yields were close to 100% and the procedure blanks were ≈17 ng, which is negligible relative to the amount of Fe loaded to the column. At least two USGS rock standards were measured during the isotope analyses of soils.

Iron isotopic ratios were analyzed by the standard bracketing method using a Neptune Plus MC-ICP–MS at the high resolution mode with mass resolution M/ΔM ≈ 8000. Iron isotope data are reported in δ-notation relative to IRMM-014: $\delta^{X}Fe(‰) = [(^{X}Fe/^{54}Fe)_{sample} / (^{X}Fe/^{54}Fe)_{IRMM\text{-}014} - 1] \times 1000$, where X = 56 or 57.

The long-term (12 months) average $\delta^{56}Fe$ of the in-house standard (UIFe) was 0.685 ± 0.048‰ (2SD, $n = 663$), and another in-house standard (GSB) was 0.719 ± 0.048‰ (2SD, $n = 391$). $\delta^{56}Fe$ of two international rock standards BHVO-2 and AGV-2 analyzed in this study are 0.10 ± 0.01 and 0.09 ± 0.03 (Table 1), respectively, agreeing well with the literature values (e.g., Craddock and Dauphas, 2011; Dauphas

Table 1
Fe isotopic compositions of USGS rock standards analyzed in this study.

Sample type	Name	δ^{56}Fe	2SD	n	δ^{57}Fe	2SD	n	δ^{56}Fe[a]	δ^{57}Fe[a]
Basalt, USA	BHVO-2	0.10	0.01	4	0.21	0.07	4	0.11 ± 0.01	0.17 ± 0.02
Andesite, USA	AGV-2	0.09	0.03	4	0.11	0.08	4	0.11 ± 0.01	0.15 ± 0.02

n, repeat measurements of a sample solution.
[a] Recommended value from Craddock and Dauphas (2011).

and Rouxel, 2006; He et al., 2015). All samples including geostandards analyzed in this study define the mass fractionation line in three-isotope space (δ^{57}Fe vs. δ^{56}Fe) with a slope of 1.494 ± 0.137 (1σ), consistent with the theoretical kinetic and equilibrium fractionation values for Fe isotopes (1.487 and 1.474, respectively) (Young et al., 2002).

Mineral compositions of the soils were measured on a BRUKER D8 ADVANCE diffractometer in the Guangzhou Institute of Geochemistry, CAS. XRD patterns of the samples were recorded between 3° and 85° (2θ) at a scanning speed of 4°/min with Cu Kα radiation (30 mA and 40 kV). The results are reported in Table 2.

Fresh laterite and peridotite samples were first powdered to < 200 μm and then dried at ≈100 °C to remove absorbed water for elemental analysis. Major elements were measured using a Rigaku ZSX100e X-ray fluorescence (XRF) spectrometer at ALS Chemex Co Ltd. Trace elements were measured using a Perkin-Elmer Elan 6100 DRC ICP–MS at the CAS Key Laboratory of Crust–Mantle Materials and Environments, USTC. Analytical procedures were described in Hou and Wang (2007). The reproducibility was better than 5% for elements with concentrations >10 ppm and better than 10% for those <10 ppm as monitored by USGS standard materials. For the weathering laterite samples, most of the Na_2O, CaO, and K_2O are close to the detection limits of XRF. Some conservative trace elements (such as Nb, U, and Zr) also become mobile during the extreme weathering process of peridotite so that the contents of some trace elements are too low to be measured. Both major- and trace-element analytical results are presented in Table 3.

4. Results

4.1. Elemental compositions

Fe_2O_3(T) (32.1–73.3 wt%) and Al_2O_3 (4.3–25.0 wt%) are obviously enriched in the weathering products, which are around three to five fold higher than the peridotites. SiO_2 concentrations in the top 2 m of the profile (6.3–24.9 wt%) are lower than those in the fresh peridotites, and they show a decreasing trend in the lower section from 3 m to 6 m (2.30 wt% to 10.51 wt%) compared with the protolith (38 wt%) (Fig. 3). MgO content of the laterite (0.43–5.13 wt%) is also dramatically lower than in the fresh peridotites (≈40 wt%).

Laterites formed in tropical or subtropical climate can produce mineral deposits. The major mineral element Ni ranges from 600 to 4600 ppm, specifically enriched in the bottom (layer IV) of the profile (Fig. 3). The abundances of most trace elements are higher in the lower section than in the upper section, whereas Rb, Zr, and Nb are enriched or less depleted in the section above 2 m (Table 3).

In the tropics, the chemical index of alteration (CIA) and intensity of chemical weathering (CIW) cannot be used to indicate the weathering degree because the calculated fluid-mobile elements such as K, Ca, and Na can easily migrate out from the weathered crust (Nesbitt and Wilson, 1992; Patino et al., 2005). As a result, these values, like CIA and CIW, are almost 100% in this profile. The high concentrations of Al_2O_3 and Fe_2O_3 (maximum values up to 24% and 73%, respectively) suggest that the chemical weathering intensity in the studied profile has been subjected to extreme weathering (Nesbitt and Wilson, 1992).

4.2. Fe isotope compositions

Fe isotopic compositions of the peridotite and saprolites from the Surigao profile are reported in Table 3. The peridotite sample has $\delta^{56}Fe = -0.03‰$, consistent with the values of global peridotites (Beard et al., 2003; Dauphas et al., 2010; Weyer and Schwieters, 2003; Zhao et al., 2012). The saprolites display a limited range of δ^{56}Fe from −0.03‰ to +0.10‰ ($n = 20$), slightly heavier than the protolith (Fig. 4a). In detail, the gravel layer and homogeneous fine laterite layer show a limited variation of δ^{56}Fe (−0.03‰ to +0.05‰). Notably, a marked increase (+0.10‰) is found in the transition horizon (5.9 m) between the fine laterite and the core stone laterite, corresponding to the decreasing trend in Fe losses ($\tau_{Ti,Fe} \approx -75\%$ to −25%) (Fig. 4b).

Table 2
Mineral proportion (wt%) of the laterite profile.

	Goethite	Hematite	Illite	Serpentine
Pili1	63.7		36.3	
Pili2	44.3		55.7	
Pili3	65.7	14.1	20.2	
Pili4	65	24.4	10.7	
Pili5	72.9	27.1		
Pili6	47.8	52.2		
Pili7	40.4	59.6		
Pili8	42.7	57.3		
Pili9	51.7	48.3		
Pili10	47.8	52.2		
Pili11	63.4	36.6		
Pili12	35	65		
Pili13	35.9	64.1		
Pili14	61	39		
Pili15	43.8	56.2		
Pili16	42.7	57.3		
Pili17	23.4	76.6		
Pili18	25.8	74.2		
Pili19		13.7		86.3
Pili20		14.6		85.4
Pili21		14.4		85.6

Sample Pili21 is peridotite and other samples are laterites.

5. Discussion

5.1. Element mobilization and distribution in the laterite

The weathering of ultramafic rocks can significantly affect mobilization and redistribution of elements, which plays an important role in the global mineral resource economy. For example, the laterites developed in conditions such as those of the Surigao can be used as Ni deposits (e.g., De Waal, 1970; Kühnel et al., 1978; Santos-Ynigo, 1964; Zeissink, 1969). Thus, it is important to investigate the mechanism of element enrichment based on the distribution of major and trace elements along the vertical profile.

Mg and Fe are enriched in the bottom (IV) and fine laterite layer (III) of the profile, respectively (Fig. 3). The results of XRD analyses show that the core stone laterite layer contains serpentine (Table 2). Thus, the Mg enrichment in the bottom of the laterite profile is possibly due to existence of lizardites forming from hydrothermal alteration of forsterites. Nahon et al. (1982a) suggested that the lizardite forms from a simple hydrolysis process, in which fluid-mobile Mg is removed to the bottom of the profile through the fissures and cracks in the layers. In contrast, the homogeneous fine laterite layer (III) shows a sharp

Table 3
Major-trace element concentrations and $\delta^{56}Fe$ of laterites and peridotite from Surigao, Philippines.

Sample	Depth (m)	Fe_2o_3 (wt%)	MgO (wt%)	Al_2O_3 (wt%)	SiO_2 (wt%)	Ni (ppm)	Cr (ppm)	Rb (ppm)	Sr (ppm)	Ba (ppm)	Zr (ppm)	Nb (ppm)
Pili1	0.6	32.14	0.46	22.24	22.92	642	1935	0.38	8.48	25.71	27.27	1.14
Pili2	1.0	27.86	0.45	24.99	24.90	613	1514	0.45	6.46	52.17	32.64	1.25
Pili3	1.4	33.31	0.48	22.72	21.92	741	2410	0.42	9.17	37.63	27.22	1.16
Pili4	2.0	60.05	0.39	13.27	6.32	1552	2447	0.19	0.81	9.27	12.12	0.61
Pili5	2.6	70.47	0.46	8.17	2.42	2225	3395	0.13	0.36	7.46	5.54	0.29
Pili5[b]												
Pili6	3.4	71.41	0.43	8.26	2.30	2609	3198	0.12	0.34	2.89	5.15	0.28
Pili7	3.8	70.69	0.64	8.63	3.18	2762	3092	0.18	0.40	5.69	5.31	0.28
Pili8	4.2	69.24	0.65	9.03	3.72	2429	4327	0.18	0.44	4.44	4.35	0.22
Pili9	4.6	68.10	0.72	9.18	4.26	2617	4457	0.20	0.42	7.99	4.59	0.20
Pili10	4.8	65.90	0.73	9.66	5.81	2618	6068	0.23	0.48	8.44	5.16	0.20
Pili11	5.1	63.92	0.54	9.08	7.03	2302	3749	0.24	0.47	2.88	3.92	0.18
Pili12	5.3	72.69	0.78	6.33	3.89	3271	5181	0.16	0.47	4.28	2.12	0.10
Pili13	5.4	73.28	0.86	6.13	4.34	2905	4545	0.13	0.39	2.70	1.55	0.07
Pili14	5.5	58.88	0.92	9.13	10.51	2425	3531	0.22	1.03	6.61	4.18	0.18
Pili15	5.6	67.43	1.00	7.46	7.16	3107	5452	0.17	0.61	3.46	2.12	0.08
Pili16	5.9	64.16	1.37	7.81	8.79	2816	5525	0.12	0.73	6.68	0.67	0.03
Pili16[b]												
Pili17	6.0	53.86	3.35	4.30	19.17	4569	4153	0.14	1.39	13.86	0.51	0.01
Pili18	6.2	49.83	5.13	4.40	20.82	4671	2747	0.13	1.94	15.23	0.21	0.01
Pili18[b]												
Pili19	6.4	13.10	29.14	1.08	38.41	2825	1027	0.07	0.91	5.15	0.17	0.00
Pili20	6.8	13.23	28.84	0.89	38.72	3804	998	0.07	1.00	4.71	0.04	0.00
Pili21	7.2	12.88	29.14	0.61	38.97	3130	1120	0.06	0.64	3.89	0.10	0.00

Sample	Depth (m)	Ti (ppm)	$\tau_{Ti,Fe}$ (%)	SiO_2/Al_2O_3	$\delta^{56}Fe$	2SD[a]	$\delta^{57}Fe$	2SD[a]
Pili1	0.6	1.72	−97.8	1.0	0.02	0.01	0.02	0.03
Pili2	1.0	1.92	−98.3	1.0	0.02	0.02	0.03	0.03
Pili3	1.4	1.64	−97.6	1.0	0.01	0.04	0.03	0.01
Pili4	2.0	0.82	−91.4	0.5	−0.01	0.02	0.02	0.01
Pili5	2.6	0.42	−80.1	0.3	0.00	0.03	0.01	0.04
Pili5[b]					0.03	0.02	0.07	0.03
Pili6	3.4	0.42	−80.2	0.3	0.00	0.03	0.04	0.10
Pili7	3.8	0.44	−81.1	0.4	−0.03	0.02	−0.05	0.06
Pili8	4.2	0.40	−79.6	0.4	0.03	0.03	0.02	0.04
Pili9	4.6	0.40	−79.7	0.5	0.01	0.03	0.03	0.03
Pili10	4.8	0.42	−81.3	0.6	0.02	0.01	0.04	0.03
Pili11	5.1	0.31	−75.4	0.8	0.00	0.05	0.04	0.08
Pili12	5.3	0.20	−57.3	0.6	−0.01	0.03	0.01	0.05
Pili13	5.4	0.17	−49.7	0.7	0.02	0.04	0.02	0.05
Pili14	5.5	0.30	−76.7	1.2	0.05	0.04	0.04	0.09
Pili15	5.6	0.1	−58.0	1.0	0.05	0.03	0.08	0.10
Pili16	5.9	0.16	−51.3	1.1	0.10	0.04	0.16	0.02
Pili16[b]					0.09	0.04	0.10	0.07
Pili17	6.0	0.08	−24.2	4.5	0.02	0.03	0.01	0.02
Pili18	6.2	0.06	−2.7	4.7	−0.02	0.04	−0.02	0.10
Pili18[b]					−0.01	0.04	0.00	0.05
Pili19	6.4	0.02	−38.0	35.6	0.05	0.03	0.12	0.06
Pili20	6.8	0.01	15.6	43.5	0.00	0.04	−0.01	0.05
Pili21	7.2	0.02	0	63.9	−0.03	0.02	−0.05	0.05

Sample Pili21 is peridotite and other samples are laterites. $\tau_{Ti,j} = 100 \times [(C_j/C_{Ti})_{saprolite} / (C_j/C_{Ti})_{protolith} - 1]$, where j refers to mobile element. $Fe_2O_3(T)$ is total Fe.
[a] 2SD was calculated based on repeated measurements by MC-ICP-MS for three times.
[b] Refers to replicate that is repeated sample dissolution, column chemistry and measurement of isotope ratio.

increase of iron content corresponding to a significant depletion of Mg, Al, and Si (Fig. 3). Under the warm and oxidizing weathering conditions, Fe should be completely transformed into ferric Fe, which is further precipitated with hematite and goethite as the dominant Fe phases in the Surigao profile (Table 2). However, Si, Mg, and mobile elements are released by the dissolution of silicates and drained away from this layer during weathering.

To evaluate quantitatively the relative depletion or enrichment of an element during chemical weathering, we calculated the percentage changes of elemental ratios to Ti relative to parent rock, $\tau_{Ti,j}$ ($\tau_{Ti,j} = 100 \times [(C_j / C_{Ti})_s / (C_j / C_{Ti})_p - 1]$, where C_j and C_{Ti} represent the concentration of elements j and Ti, respectively, and "s" and "p" refer to saprolite and parent rock, Nesbitt and Markovics (1980)). Titanium is used as a conservative element here because it is resistant to acidic environment in the basaltic weathering profiles (Hill et al., 2000; Nesbitt and Markovics, 1980). Positive or negative $\tau_{Ti,j}$ values indicate enrichment or depletion of element j relative to the parent rock, respectively. Most samples display distinguishable $\tau_{Ti,Fe}$ (−50% to −70%), while the gravel layer samples have notably negative $\tau_{Ti,Fe}$ (−91% to −98%), showing that Fe was obviously lost from almost all of the layers. With the extreme weathering intensity, most of the elements such as K, Ca, Na, and Mg are almost entirely lost from the profile. Fe is less mobile because the most iron released from the parent rock was oxidized to Fe^{3+} with low solubility. So Fe was enriched or less depleted compared to these mobile elements in laterites, even though it was also significant lost according to the $\tau_{Ti,Fe}$ values.

Moreover, we observed that the highest Ni content occurs in the upper part of the laterite with a core stone layer while the highest Cr content occurs in the bottom of the homogeneous fine laterite layer (Table 3 and Fig. 3). It has been suggested that forsterites are the Ni-bearing minerals, while enstatites are Cr-bearing minerals (Nahon et al., 1982b). Talc and smectites are generated by weathering of forsterites and enstatites, respectively. Therefore they are concentrated in Ni and Cr (Nahon et al., 1982a).

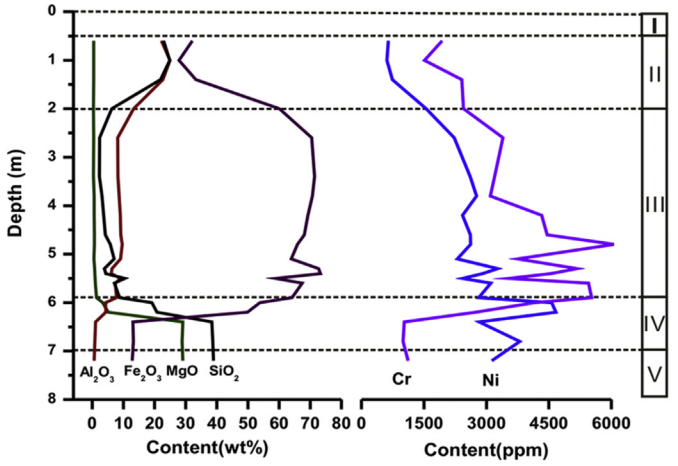

Fig. 3. The compositional variations of Fe, Al, Mg, Si, Cr, and Ni relative to the protolith along the weathering profile. The layer designations are: I, topsoil; II, gravel layer; III, homogeneous fine laterite layer; IV, laterite with core stone; and V, peridotite.

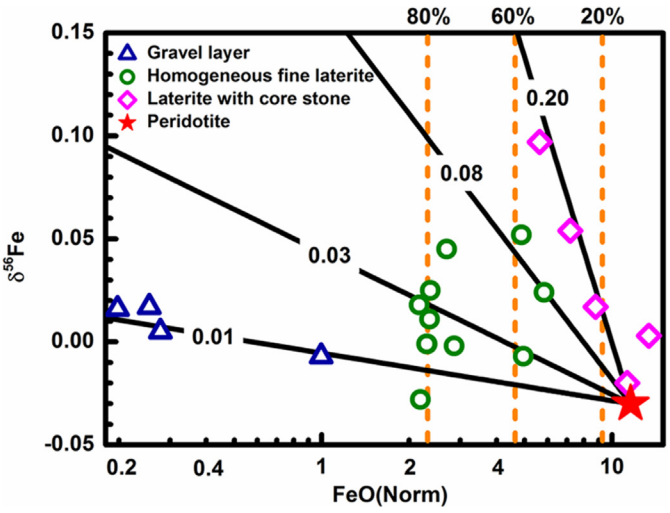

Fig. 5. Correlation of $\delta^{56}Fe$ with iron concentration normalized to titanium. Solid lines depict Fe removal via Rayleigh distillation with different fractionation factor $10^3\ln\alpha$ [$\alpha = (^{56}Fe/^{54}Fe)_{saprolite} / (^{56}Fe/^{54}Fe)_{fluid}$]. $\delta^{56}Fe_{saprolite} = (\delta^{56}Fe_{peridotite} + 1000)f^{(\alpha-1)} - 1000$, where f is the fraction of Fe remaining in the rock as calculated from $Fe_{saprolite}/Fe_{peridotite}$. Star represents peridotite; triangles represent samples at gravel layer; open circles represent samples at homogeneous fine laterite; and diamonds are samples at laterite with core stone. Vertical dashed lines indicate the relative percentage of sample Fe loss.

5.2. Fe isotope fractionation along the laterite profile

Despite the large Fe losses by ~50% to 90% according to the $\tau_{Ti,Fe}$ factors (Fig. 4b), their $\delta^{56}Fe$ variations along the whole vertical profile are limited (0.13‰) (Fig. 4a). Consequently, our results are consistent with the previous studies that extreme weathering and significant Fe lost may only induce limited Fe isotopic variation in laterites (Liu et al., 2014; Poitrasson et al., 2008). We have adopted a Rayleigh distillation model to simulate the relationship between Fe loss and Fe isotope fractionation. Light Fe isotopes prefer fluids to saprolites with an apparent $10^3\ln\alpha$ [$\alpha = (^{56}Fe/^{54}Fe)_{saprolite} / (^{56}Fe/^{54}Fe)_{fluid}$] varying from 0.01 to 0.20 (Fig. 5). These values are much smaller than the fractionation factors experimentally determined for reductive dissolution of goethite ($10^3\ln\alpha_{goethite\text{-}Fe(II)} \approx 1.2$; Icopini et al., 2004) and hematite ($10^3\ln\alpha_{hematite\text{-}Fe(II)} \approx 1.3$; Beard et al., 2003). Therefore, the mechanism for Fe isotope fractionation and Fe loss in tropical weathering systems is fundamentally different from the reductive dissolution of iron oxides. It is also possible that proton-promoted dissolution does not cause measurable iron isotope fractionation during the laterite formation process (Wiederhold et al., 2006). However, the pH of acid required to dissolve Fe^{3+}-bearing minerals is too low for the soils. For example, the proton-promoted (HCl) dissolution experiments of goethite in Wiederhold et al. (2006) used HCl with pH of 0.3, much lower than the typical laterite pH value ~4–6 (Gidigasu, 2012). Thus, proton-promoted dissolution is not a major factor for Fe isotope fractionation in the Surigao laterite.

It is difficult to evaluate how dissolution and leaching of Fe-bearing minerals modulated Fe isotopic composition of the saprolites because most of the primary minerals reacted out. However, the consistent slopes of the Rayleigh distillation lines for the three layers (Fig. 5) indicate that variations in iron isotopic compositions are still resolvable in tropical or subtropical laterites and among diverse weathering intensity horizons. Because the $10^3\ln\alpha$ values are much smaller than the fractionation factors experimentally determined for reductive dissolution of the Fe-bearing mineral hosts (e.g., goethite and hematite), these values would not represent the effect of the reductive iron elemental exchanges. In this view, this is clearly related to strong transformations of Fe-bearing minerals during tropical weathering and laterite formation.

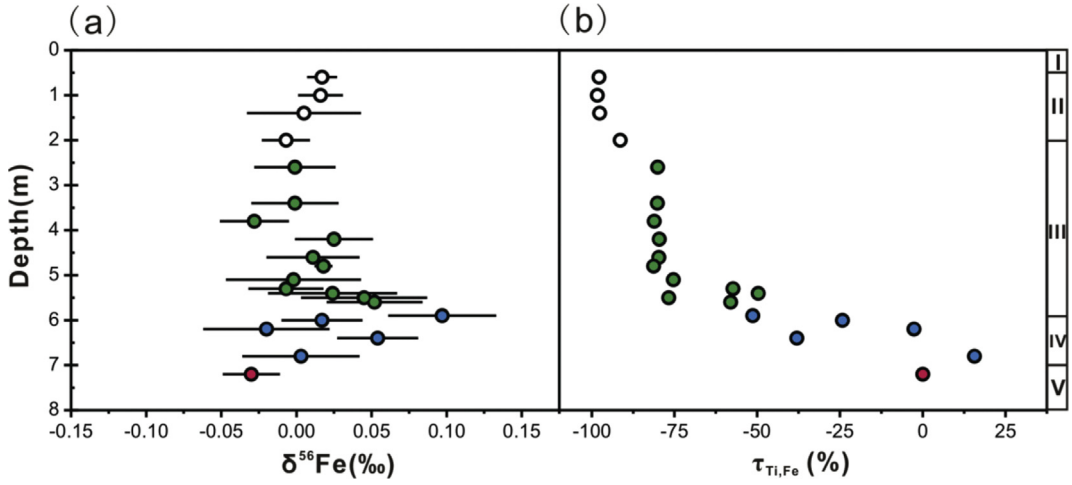

Fig. 4. (a) $\delta^{56}Fe$ and (b) $\tau_{Ti,Fe}$ as a function of depth in the weathering profile. Error bars represent 2 standard deviation. The layer I, II, III, IV, and V are similar to Fig. 3.

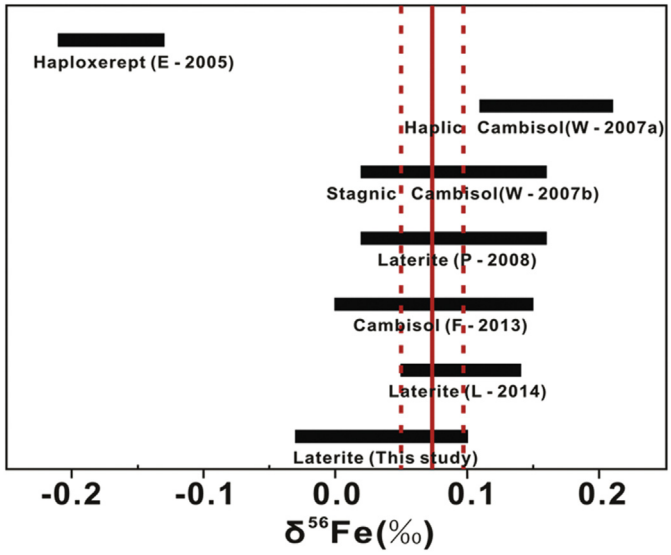

Fig. 6. Range of δ^{56}Fe in bulk soil samples from worldwide. Compared to other soils previously studied, twenty laterite samples from Surigao, Philippines show a small range of Fe isotope variations similar to the continental crust mean value (Poitrasson, 2006). Soils in the literature are from Cameroon (P-2008. Poitrasson et al., 2008), China (L-2014. Liu et al., 2014), France (F-2013. Fekiacova et al., 2013), Germany (W-2007a. Wiederhold et al., 2007a), Switzerland (W-2007b. Wiederhold et al., 2007b) and Israel (E-2005. Emmanuel et al., 2005). Vertical dashed lines represent δ^{56}Fe of the continent crust (Poitrasson, 2006).

5.3. The limited Fe isotopic variations in other soils

The dramatic loss of Fe in the laterite profile and limited Fe isotope fractionation provide important information for studying Fe transfer in soils and soil evolution. It allows us to evaluate the behavior of Fe in the near-surface environment during pedogenesis and to investigate evolution processes of soil (e.g., Fantle and DePaolo, 2004; Poitrasson et al., 2008; Wiederhold et al., 2007a). To understand such observation, we have compiled the Fe isotope data showing limited fractionation in the profile ($\Delta^{56}Fe_{profile}$ < 0.15‰) from a number of soil profiles published in the literature. The overall range for the bulk soils is −0.21‰ to +0.16‰ (Fig. 6). The soils can be divided into two groups on the basis of the common characteristics of formation environment.

Group 1 consists of cambisols and laterites. They are developed under oxic and well-drained conditions with a dominantly vertical water transfer. The lack of Fe isotopic fractionation in the profile could be due to limited transport of Fe^{3+} via water circulation because of the low solubility of Fe^{3+}-bearing minerals such as goethite and hematite (Poitrasson et al., 2008). Or alternatively, it could be due to that the Fe released from mineral dissolution may in situ precipitate to form secondary minerals, as suggested by Wiederhold et al. (2007a).

Group 2 soils are mainly haplic gleysols and the stagnic combisols with a similar range of δ^{56}Fe to group 1. In contrast to the forming conditions of the group 1 soils, the group 2 soils form in water-saturated and reduced conditions (Wiederhold et al., 2007b). Because reductive Fe mobilization under anoxic state was inferred to occur in the studied soils and the mobile fraction in soils in general has lighter Fe isotopic composition (Brantley et al., 2004; Fantle and DePaolo, 2004; Thompson et al., 2007), the restricted Fe isotopic variations may imply that the transport of Fe within the soil was spatially limited. Therefore, most Fe could be transferred only at the scale of a few millimeters or less so that significant Fe isotope variations cannot be observed in the reduced soils (Wiederhold et al., 2007b).

To conclude, in the oxidized situations, the small Fe isotope fractionation in the whole profile suggests that after iron released from the parent rock was oxidized to Fe^{3+}, the subsequent Fe mobility was limited due to the low solubility of the host minerals (goethite and hematite). In reductive situations, limited Fe isotope fractionation suggests that transport of aqueous Fe^{2+} species should be spatially limited (such as within millimeter scales).

5.4. Implications for Fe cycling during lateritic weathering

Mobilization of Fe in soils can be accompanied by notable Fe isotope fractionation if Fe^{2+} is mobilized by water and organic acids or oxides are partially reduced (e.g., Emmanuel et al., 2005; Fantle and DePaolo, 2004) (Fig. 7a). In contrast, the restricted δ^{56}Fe variation and significant iron loss of the laterite profiles can be explained by entire and in situ oxidation in tropical weather. In this case, the primary Fe-bearing minerals

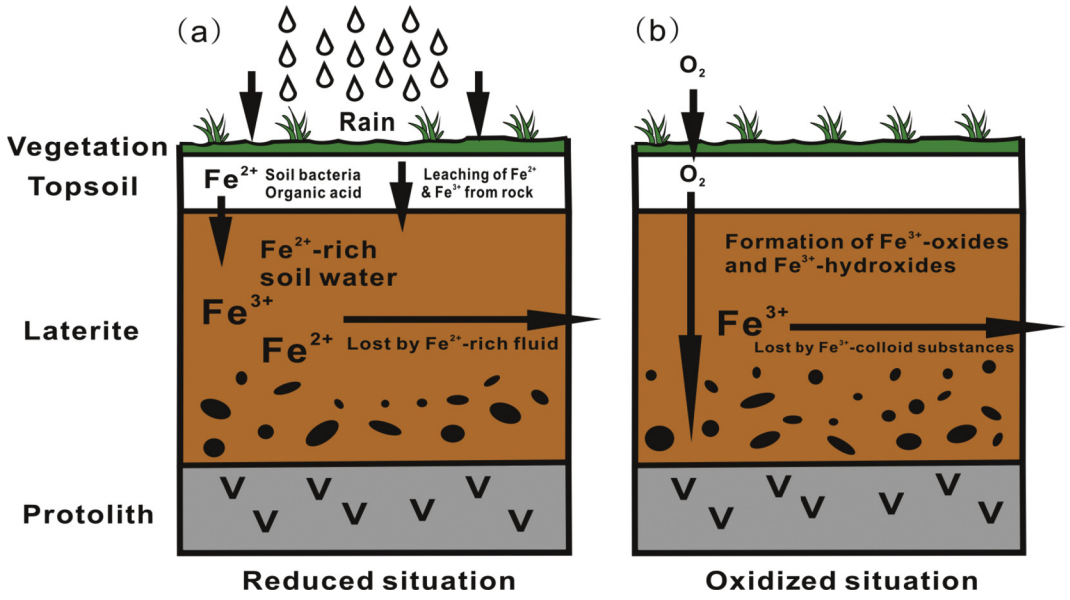

Fig. 7. A schematic model showing laterite formation process. (a) Under reduced situation, removal of Fe with low δ^{56}Fe through mobilization by water, organic acids and/or Fe^{3+}-reducing bacteria could produce a residue with heavy δ^{56}Fe. (b) Under the oxidized situation, infiltrating atmospheric O_2 produces Fe^{3+}-oxides and/or Fe^{3+}-hydroxides. Migration of Fe^{3+} via colloid substances can lose large amount of Fe without significant fractionation of Fe isotopes.

decomposed and Fe was released from the minerals. Due to the high oxygen fugacity in the tropical environment, a large amount of free oxygen enter from the atmosphere into the soil through dry porous surfaces, cracks, and fissures of the profile so that the oxidative process could be rapid (Yamaguchi et al., 2007) (Fig. 7b). Therefore, when Fe^{2+} encounters O_2, it is completely oxidized to Fe^{3+} which further precipitates into Fe^{3+}-oxides and Fe^{3+}-hydroxides.

As noted in Section 5.3, Fe^{3+} is not mobile in water to induce significant Fe loss. Therefore, the most possible explanation for the negative $\tau_{Ti,Fe}$ could be associated with ferric iron colloids. The positively charged iron colloidal materials can be vigorously attached to negatively charged clay particles and they are leached together (Gidigasu, 2012; Maignien, 1966). Ferric iron can therefore be associated with certain substances passing through soils. The variations of $\delta^{56}Fe$ in the studied profile (from −0.03 to +0.10‰) indicate that the iron isotope composition of ferric colloids is similar to the continental crust ($\delta^{56}Fe = 0.07 \pm 0.02$, Poitrasson, 2006). The results are different from previous study showing that the organo-ferric colloids from subarctic and temperate area are enriched in heavy Fe isotopes (Ilina et al., 2013). Ilina et al. (2013) also discovered a systematic difference of the correlation of $\delta^{57}Fe$ with Fe/C ratios between subarctic and temperate water samples. Therefore, they attributed the nature of environments, like the various soil/water situation and microbial activities, to control the iron isotope variations. The Surigao profile formed under tropical climate with extreme weathering and Fe loss which is different with the cases of temperate and subarctic climate. Overall, the limited iron isotope variations in the laterites suggest that ferric Fe colloids are essential for iron migration during the extreme weathering process under (sub)-tropical climate.

6. Conclusions

We report Fe isotopic compositions and element variations of a laterite profile developed from weathered peridotite from Surigao (Philippines) under a tropical climate. The elemental geochemistry of laterite profile suggests that most elements, even the general conservative ones like Fe, Zr, and Nb, become mobile during extreme weathering in tropical climate. The iron isotope results show that the lateritization process produced strong Fe loss ($\tau_{Ti,Fe} \approx -50\%$ to -90%) but limited iron isotope fractionation along the whole laterite profile (0.13‰). This observation has important implications for the geochemical cycling of Fe during laterite formation, suggesting that the studied profile should have experienced a complete and in situ oxidation before Fe migration. Finally, in order to lose Fe^{3+}, Fe was probably transferred in the form of colloid substances.

Acknowledgements

This work is supported by the National Science Foundation of China (41571130052, 41325011, 41503001), the 111 Project, and the Fundamental Research Funds for the Central Universities. We are grateful to Ya Gao for providing the laterite samples from the Surigao weathering profile. Yu-Han Qi, Tian-Tian Wang, Hong-Jie Wu, Juan Xu, Xing-Chao Zhang, Ying-Zeng Gong, Zhen-Hui Hou, Shi-Chao An, and Yue Zhang are thanked for help in laboratory. We are grateful to Chen Zhou, Fei Wu, Hong-Luo Zhang, and Ya-Jun An for discussion. We also thank A.B. McBratney for editorial handling and two anonymous referees for their constructive comments on the paper.

References

Beard, B.L., et al., 2003. Application of Fe isotopes to tracing the geochemical and biological cycling of Fe. Chem. Geol. 195 (1), 87–117.
Brantley, S.L., et al., 2004. Fe isotopic fractionation during mineral dissolution with and without bacteria. Geochim. Cosmochim. Acta 68 (15), 3189–3204.
Braxton, D.P., Cooke, D.R., Ignacio, A.M., Rye, R.O., Waters, P.J., 2009. Ultra-deep oxidation and exotic copper formation at the late Pliocene Boyongan and Bayugo porphyry copper-gold deposits, Surigao, Philippines: geology, mineralogy, paleoaltimetry, and their implications for geologic, physiographic, and tectonic controls. Econ. Geol. 104 (3), 333–349.
Bullen, T.D., White, A.F., Childs, C.W., Vivit, D.V., Schulz, M.S., 2001. Demonstration ofsignificant abiotic iron isotope fractionation in nature. Geology 29, 699–702.
Chapman, J.B., Weiss, D.J., Shan, Y., Lemburger, M., 2009. Iron isotope fractionation during leaching of granite and basalt by hydrochloric and oxalic acids. Geochim. Cosmochim. Acta 73 (5), 1312–1324.
Craddock, P.R., Dauphas, N., 2011. Iron isotopic compositions of geological reference materials and chondrites. Geostand. Geoanal. Res. 35 (1), 101–123.
Dauphas, N., Rouxel, O., 2006. Mass spectrometry and natural variations of iron isotopes. Mass Spectrom. Rev. 25 (4), 515–550.
Dauphas, N., Teng, F.-Z., Arndt, N.T., 2010. Magnesium and iron isotopes in 2.7 Ga Alexo komatiites: mantle signatures, no evidence for Soret diffusion, and identification of diffusive transport in zoned olivine. Geochim. Cosmochim. Acta 74 (11), 3274–3291.
De Waal, S., 1970. Nickel minerals from Barberton, South Africa: III. Willemseite, a nickel-rich talc. Am. Mineral. 55 (1–2), 31–42.
Emmanuel, S., Erel, Y., Matthews, A., Teutsch, N., 2005. A preliminary mixing model for Fe isotopes in soils. Chem. Geol. 222 (1), 23–34.
Fantle, M.S., DePaolo, D.J., 2004. Iron isotopic fractionation during continental weathering. Earth Planet. Sci. Lett. 228 (3), 547–562.
Fekiacova, Z., Pichat, S., Cornu, S., Balesdent, J., 2013. Inferences from the vertical distribution of Fe isotopic compositions on pedogenetic processes in soils. Geoderma 209, 110–118.
Gidigasu, M., 2012. Laterite Soil Engineering: Pedogenesis and Engineering Principles, 9. Elsevier.
He, Y., et al., 2015. High-precision iron isotope analysis of geological reference materials by high-resolution MC-ICP-MS. Geostand. Geoanal. Res. 39 (3), 341–356.
Hill, I., Worden, R., Meighan, I., 2000. Yttrium: the immobility-mobility transition during basaltic weathering. Geology 28 (10), 923–926.
Hou, Z.-h., Wang, C.-x., 2007. Determination of 35 trace elements in geological samples by inductively coupled plasma mass spectrometry. Journal of University of Science and Technology of China 37, 940–944.
Huang, F., Zhang, Z., Lundstrom, C.C., Zhi, X., 2011. Iron and magnesium isotopic compositions of peridotite xenoliths from Eastern China. Geochim. Cosmochim. Acta 75 (12), 3318–3334.
Icopini, G., Anbar, A., Ruebush, S., Tien, M., Brantley, S., 2004. Iron isotope fractionation during microbial reduction of iron: the importance of adsorption. Geology 32 (3), 205–208.
Ilina, S.M., et al., 2013. Extreme iron isotope fractionation between colloids and particles of boreal and temperate organic-rich waters. Geochim. Cosmochim. Acta 101, 96–111.
Johnson, C.M., Beard, B.L., Roden, E.E., Newman, D.K., Nealson, K.H., 2004. Isotopic constraints on biogeochemical cycling of Fe. In: Geochemistry of Non-Traditional Stable Isotopes. Reviews in mineralogy and geochemistry. No.55. Mineralogical Society of America, Washington, DC, pp. 359–408.
Kühnel, R., Roorda, H., Steensma, J., 1978. Distribution and partitioning of elements in nickeliferous laterites. Bull. BRGM 2 (3), 191–206.
Liermann, L.J., et al., 2011. Extent and isotopic composition of Fe and Mo release from two Pennsylvania shales in the presence of organic ligands and bacteria. Chem. Geol. 281 (3–4), 167–180.
Liu, S.-A., et al., 2014. Copper and iron isotope fractionation during weathering and pedogenesis: insights from saprolite profiles. Geochim. Cosmochim. Acta 146, 59–75.
Maignien, R., 1966. Review of Research in Laterites.
Nahon, D.B., Paquet, H., Delvigne, J., 1982a. Lateritic weathering of ultramafic rocks and the concentration of nickel in the western Ivory Coast. Econ. Geol. 77 (5), 1159–1175.
Nahon, D., Colin, F., Tardy, Y., 1982b. Formation and distribution of Mg, Fe, Mn-smectites in the first stages of the lateritic weathering of forsterite and tephroite. Clay Miner. 17 (3), 339–348.
Nesbitt, H.W., Markovics, G., 1980. Chemical processes affecting alkalis and alkaline earths during continental weathering. Geochim. Cosmochim. Acta 44 (11), 1659–1666.
Nesbitt, H., Wilson, R., 1992. Recent chemical weathering of basalts. Am. J. Sci. 292 (10), 740–777.
Patino, L.C., Velbel, M.A., Price, J.R., Wade, J.A., 2005. Element redistribution during weathering of volcanic rocks in sedentary landscapes. Geochimica et Cosmochimica Acta Supplement 69, 683.
Poitrasson, F., 2006. On the iron isotope homogeneity level of the continental crust. Chem. Geol. 235 (1), 195–200.
Poitrasson, F., Viers, J., Martin, F., Braun, J.-J., 2008. Limited iron isotope variations in recent lateritic soils from Nsimi, Cameroon: implications for the global Fe geochemical cycle. Chem. Geol. 253 (1), 54–63.
Santos-Ynigo, L., 1964. Distribution of Iron, Alumina and Silica in the Pujada Laterite of Mati, Davao Province, Míndanao Island (Phillipines), 22 International Geological Congress.
Skulan, J.L., Beard, B.L., Johnson, C.M., 2002. Kinetic and equilibrium Fe isotope fractionation between aqueous Fe (III) and hematite. Geochim. Cosmochim. Acta 66 (17), 2995–3015.
Tardy, Y., 1997. Petrology of Laterites and Tropical Soils. AA Balkema.
Thompson, A., Ruiz, J., Chadwick, O.A., Titus, M., Chorover, J., 2007. Rayleigh fractionation of iron isotopes during pedogenesis along a climate sequence of Hawaiian basalt. Chem. Geol. 238 (1), 72–83.
Weyer, S., Schwieters, J., 2003. High precision Fe isotope measurements with high mass resolution MC-ICPMS. Int. J. Mass Spectrom. 226 (3), 355–368.
Wiederhold, J.G., et al., 2006. Iron isotope fractionation during proton-promoted, ligand-controlled, and reductive dissolution of goethite. Environ. Sci. Technol. 40 (12), 3787–3793.
Wiederhold, J.G., Teutsch, N., Kraemer, S.M., Halliday, A.N., Kretzschmar, R., 2007a. Iron isotope fractionation in oxic soils by mineral weathering and podzolization. Geochim. Cosmochim. Acta 71 (23), 5821–5833.
Wiederhold, J.G., Teutsch, N., Kraemer, S.M., Halliday, A.N., Kretzschmar, R., 2007b. Iron isotope fractionation during pedogenesis in redoximorphic soils. Soil Sci. Soc. Am. J. 71 (6), 1840–1850.

Yamaguchi, K.E., et al., 2007. Isotopic evidence for iron mobilization during Paleoproterozoic lateritization of the Hekpoort paleosol profile from Gaborone, Botswana. Earth Planet. Sci. Lett. 256 (3), 577–587.
Yesavage, T., et al., 2012. Fe cycling in the Shale Hills critical zone observatory, Pennsylvania: an analysis of biogeochemical weathering and Fe isotope fractionation. Geochim. Cosmochim. Acta 99, 18–38.
Young, E.D., Galy, A., Nagahara, H., 2002. Kinetic and equilibrium mass-dependent isotope fractionation laws in nature and their geochemical and cosmochemical significance. Geochim. Cosmochim. Acta 66 (6), 1095–1104.
Zeissink, H., 1969. The mineralogy and geochemistry of a nickeliferous laterite profile (Greenvale, Queensland, Australia). Mineral. Deposita 4 (2), 132–152.
Zhao, X., Zhang, H., Zhu, X., Tang, S., Yan, B., 2012. Iron isotope evidence for multistage melt–peridotite interactions in the lithospheric mantle of eastern China. Chem. Geol. 292, 127–139.